Carrier Mobility Dynamics under Actual Working Conditions of Organic Solar Cells

Rokas Jasiuunas, Vidmantas Jasinskas, Huotian Zhang, Tanvi Upreti, Feng Gao, Martijn Kemerink and Vidmantas Gulbinas

Jasiuunas, R., Jasinskas, V., Zhang, H., Upreti, T., Gao, F., Kemerink, M., Gulbinas, V., (2021), Carrier Mobility Dynamics under Actual Working Conditions of Organic Solar Cells, *The Journal of Physical Chemistry C*, 125(27), 14567-14575. https://doi.org/10.1021/acs.jpcc.1c04245

Carrier Mobility Dynamics at Actual Working Conditions of Organic Solar Cells

*Rokas Jasiūnas**[1], Vidmantas Jašinskas[1], Huotian Zhang[2], Tanvi Upreti[2,3], Feng Gao[2], Martijn Kemerink[2,3] and Vidmantas Gulbinas[1]*

[1] Center for Physical Sciences and Technology, Sauletekio av.3, Vilnius, 10257, Lithuania

[2] Department of Physics Chemistry and Biology (IFM), Linköping University, Linköping SE-58183, Sweden

[3] Centre for Advanced Materials, Ruprecht-Karls-Universität Heidelberg, Im Neuenheimer Feld 225, D-69120 Heidelberg, Germany

Corresponding Author

rokas.jasiunas@ftmc.lt

ABSTRACT. Though organic photovoltaics has made significant progress since its appearance decades ago, the underlying physics of charge transport in working cells is still under debate. Carrier mobility, determining their extraction and recombination is one of the most important, but complex and still poorly understood parameters. Low energy charge carrier states acting as traps play a particularly important role in carrier transport. Occupation of these states in real operation conditions of solar cells induces additional complexity. In this work, we use several transient methods and numerical modelling to address carrier transport in actual working conditions of bulk-heterojunction organic solar cells based on fullerene and non-fullerene acceptors. We show that occupation of low-energy states strongly depends on the blend materials and the effective electric field. We define conditions when such occupation increases carrier mobility, making it less time-dependent on μs time scale, and when its influence is only marginal. We also show that the initial mobility, determined by carrier relaxation within high energy part of distributed density of states, strongly decreases with time independently of low-energy state population.

KEYWORDS: mobility, charge carrier, recombination, extraction, organic solar cells, nonfullerene

Introduction

Organic photovoltaics (OPV) has been steadily developing for more than thirty years as a promising solar-to-electrical power conversion technology[1]. Although organic solar cells have been thoroughly investigated and currently reach market-appropriate efficiencies[2,3], the underlying physics is still not fully understood.

Charge carriers photogenerated in an active layer of OPV device are either extracted, contributing to current, or recombine, which is the loss channel. These processes depend on extraction and recombination rates. The first is subject to carrier mobility, which in the general case changes with time and depends on the internal electric field. Recombination rate coefficient and carrier density determine recombination losses. Moreover, all these processes are strongly affected by the carrier trapping, which reduces carrier mobility and might enhance the fraction of recombined carriers. Therefore, high trap concentrations lead to reduced open-circuit voltage (Voc), fill factor (FF) and short-circuit current (Jsc)[4–6]. In this context, we should distinguish between the broad density of states (DOS) distribution of localized states within the bandgap that is characteristic for the disordered materials that are typically used in the OPV active layers, which are also referred to as tail states [7,8], and possible additional distributions of trap states that may be formed deep below these tail states due to impurities, defects etc. [9]. However, experimental differentiation of the tail and trap states is complicated, therefore here we address the combined effect of all low-energy states. We will analyze their influence on carrier transport, which depends on their depth, density, energetics and even spatial distribution [9-11].

Carrier extraction is directly determined by their mobility. Moreover, the recombination rate is also determined by mobility through the Einstein relation between mobility and diffusivity. Carrier mobility in organic materials usually is not constant. It depends on temperature, electric field

strength and decreases with time [12–15]. Carrier mobilities in blends of organic solar cells were also reported to decrease by several orders of magnitude from their generation until extraction [16–23]. On the other hand, there are also reports claiming that steady-state mobility analysis can be successfully applied to OPV devices[24–27]. Recently, Koster's group argued that carrier mobility in operating solar cells is indeed constant and that transient methods, where the sample is excited by a short laser pulse, are inadequate for the mobility dynamics investigation in operating solar cells, because of low-energy state occupation under steady-state illumination[28]. This work was disputed [29], but so far there is no clear experimental data to reveal the role of low-energy state population on carrier extraction and recombination. Even more, it remains unclear how and if steady-state illumination leads to a low-energy state population, hindering mobility decay.

The task of this work was to shed light on above discussed processes by comparing extraction and recombination of charge carriers generated by weak short laser pulses in either absence or presence of additional continuous illumination by 1 sun light source, imitating real solar cell operation conditions. We have investigated population of low-energy states by solar irradiation in bulk heterojunction organic solar cells with fullerene and non-fullerene acceptors and its influence on charge carrier transport. We demonstrate that low-energy state population in low efficiency solar cells becomes significant at voltages similar to those of working conditions, causing faster carrier extraction and increased recombination. In contrast, in the efficient non-fullerene solar cell, carrier trapping plays no significant role. Nevertheless, initial carrier mobility remains strongly time-dependent regardless of solar illumination even in cells with the strongest carrier trapping.

Methods.

We investigated three types of solar cells: the archetypical TQ1:$PC_{71}BM$ device, which has been exhaustively studied in recent years as a standard model of the polymer-fullerene solar cell,[30–32] PCE10:$PC_{71}BM$ devices with different donor and acceptor stoichiometric ratios and efficient non-fullerene device PBDB-T:Y1, based on record-breaking Y-series acceptor[33]. Chemical structures of the used materials and photoelectrical properties of the investigated solar cells are presented in Fig.S1 in S.I. The device fabrication procedures are also described in S.I.

To investigate the whole charge carrier extraction dynamics, starting from their generation on a sub-picosecond time scale up to their extraction during microseconds, we applied three time-resolved techniques: transient photocurrent (TPC) and time-delayed collection field (TDCF) techniques were used to address carrier motion on a nanosecond-microsecond time scale and time-resolved electric field-induced second harmonic generation (TREFISH) technique was used for ultrafast carrier motion investigation.[16,18] To address the influence of low-energy state occupation in real operation conditions, all the measurements were performed with and without an additional steady-state 1.5AM intensity illumination, which in the following will be called as 1 sun light.

Transient Photocurrent. During conventional transient photocurrent measurements, samples were excited with short laser pulses at the specific effective voltage U_{Eff}. Here the effective voltage is regarded as a sum of applied external voltage and built-in voltage, i.e. $U_{Eff} = U_{App} + U_{Built\text{-}in}$. Majority of measurements were performed at voltages below open-circuit voltage, when current flows to backward direction, therefore for convenience in the following we consider current values to be positive (voltage, respectively) when flowing in a backward direction. Electric scheme and time sequences of TPC are presented in S.I.

Samples were excited by radiation of the optical parametric amplifier Topas-C (Light Conversion Ltd.) pumped by femtosecond Ti:sapphire laser Integra-C from Quantronix Inc. generating ~150

fs duration pulses at 430 Hz repetition rate. Collinear optical parametric amplifier TOPAS-C was used to generate the excitation pulse emitting at 515 nm. Current transients were recorded by Agilent Technologies DS05054A oscilloscope (bandwidth 500MHz), voltages were set by Tektronix AFG 3101 function generator. Time resolution of the measurement were limited by the RC of the circuit equal to about 150 ns determined by the resistance of the oscilloscope and generator, and the sample capacitance.

Time-Delayed Collection Field. TDCF is specific TPC measurement implementation, where the sample is excited at zero, or low effective voltage, called generation voltage U_{GEN} and after some particular delay time strong extraction voltage U_{EXT} is applied to collect all carriers and evaluate their density. Here we assume that effective extraction voltage of 1,8V can extract all charge carriers present in the sample at its application time. Schematic representation of TDCF measurement is presented in Fig.S3. If the generation voltage is set to compensate for the internal build-in electric field, then photocurrent equals zero and carrier density during delay time before extraction decreases only because of recombination. Therefore, TDCF is one of the routine methods for investigating the carrier recombination dynamics[17,32,40,41]. TDCF measurements were performed using the same experimental setup as for TPC measurements.

Time-resolved electric field induced second harmonic. We used this ultrafast optical pump-probe technique to evaluate carrier mobility kinetics on a ps-ns time scale. It is explained in detail elsewhere[16,34]. In short, drifting charge carriers produced by a femtosecond laser pulse are screening electric field, which is probed by recording the intensity of the electric field induced second harmonic (EFISH) signal created by probe pulse applied after a variable delay. The EFISH signal depends on electric field strength quadratically. Considering active layer as an insulator sandwiched between two electrodes as a capacitor, the electric field change can then be

straightforwardly transformed into an amount of extracted charge using a simple capacitor relation: $\Delta Q = C\Delta U$. Assuming that for carriers to be extracted on average they have to travel half the thickness of an active layer, allows evaluating average carrier drift and consequently time-dependent carrier mobility. The TREFISH investigations were performed using the same femtosecond laser as TPC measurements.

Model description. Numerical modelling of carrier extraction and recombination processes was also applied for TPC and TDCF data interpretation. Transient photocurrent created by a short laser pulse may be formally expressed as:

$$j(t) = e\, n(t)\mu(t)F, \tag{1}$$

where e is the elementary charge, F electric field strength, $n(t)$ carrier density and $\mu(t)$ average carrier mobility. Therefore, photocurrent decay is determined by two time-dependent parameters: $n(t)$ and $\mu(t)$. Carrier density decays with time because of the carrier recombination and their extraction from the active layer to electrodes. Generally, the charge carrier mobility is also time-dependent because charge carriers gradually populate low-energy states within the distributed density of states and become less mobile, get trapped, and in some cases are stopped by barriers[10].

Density of charge carriers generated by laser pulse n_{laser} (in the following we call them as laser-carriers) decreases due to their recombination and extraction, and may be formally expressed as:

$$\frac{dn_{laser}}{dt} = -\gamma(t)\, {n_{laser}}^2 + \gamma(t) n_{laser} n_{Sun} - \frac{j(t)}{de} \tag{2}$$

where, $\gamma(t)$ – is bimolecular recombination rate, d – sample thickness, n_{sun} is the density of charge carriers generated by constant 1sun light (in the following we call them as sun-carriers). A fraction of sun-carriers are trapped, thus the second term also accounts for the Shockley–Read–Hall (SRH)

recombination of laser-carriers with the trapped sun-carriers. In case of measurements in absence of additional continuous illumination, the second term is absent and we ignore the SRH recombination because of weak population of low-energy states by used low intensity and low repetition rate laser pulses. Here we assumed that bimolecular recombination rate was time-dependent and proportional to time dependent mobility:

$$\gamma(t) = \beta\mu(t) \tag{4}$$

where, β - the coefficient of proportionality, which was obtained setting initial $\gamma(t)$ value to time-independent γ obtained from TDCF measurements in case of zero effective generation voltage.

Time-dependent mobility was obtained by combining transient photocurrent and TDCF measurements. For that we used an assumption, that all the extracted charge constituted to photocurrent value at the time of extraction voltage application; therefore, neglecting charge carrier losses during non-instantaneous (~few ns) extraction voltage application. Knowing $j(t)$ values from TPC measurement and $n(t)$ from TDCF, we were able to evaluate mobility values by using eq. 1.

Results and discussion

We start analysis of the experimental data with the well-established TQ1:$PC_{71}BM$ blend. Although the investigated device showed a decent PCE of 5.3%, its fill factor was only 0.39, which could be due to increased carrier trapping as compared to more conventional TQ1:$PC_{71}BM$ devices. However, for the present purpose, these samples are excellently suited to demonstrate the role of strong carrier trapping on carrier mobility and recombination dynamics.

Analysis and interpretation of the experimental results becomes simpler by using low intensity laser excitation, when we can neglect bimolecular recombination taking place between laser-carriers. Importantly, in this limit, the laser-carriers experience identical experimental conditions as sun-carriers and, thus correctly represent dynamics of individual charge carriers in real solar cell operation conditions. We determined this limit from excitation intensity dependence of photocurrent kinetics.

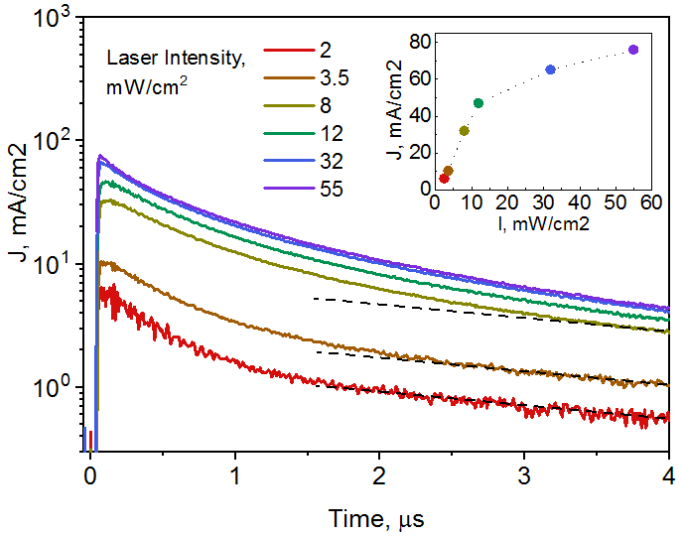

Figure 1. *Photocurrent kinetics dependence on 515nm laser excitation intensity for TQ1:$PC_{71}BM$ sample. Parallel dotted lines are guide-to-the-eye, indicating different decay rates. Inset shows peak values of photocurrent.*

Fig. 1 shows photocurrent transients at various excitation intensities measured at effective internal voltage of 0.2V, which is close to the maximal power point (MPP) of the solar cell. Several nonlinear processes are expected to take place and be responsible for the changes of the photocurrent transients at increased excitation intensity: exciton annihilation, bimolecular carrier recombination, occupation of low-energy states. At the two lowest intensity values, the current kinetics has very similar shape indicating that nonlinear processes still play only marginal role.

Therefore, the photocurrent shape during the first microsecond is mainly determined by the carrier relaxation to low-energy states within DOS, which reduces their mobility[18], while at longer times, current decays due to extraction of equilibrated charge carriers. By increasing excitation intensity, we do not observe significant changes of the current decay kinetics during the first microsecond, which could take place in case of significant occupation of low-energy states changing the carrier mobility decay. However, the photocurrent peak starts to saturate at high intensities (see inset in Fig.1), most likely due to the exciton annihilation. The photocurrent decay during 1-5 microseconds also becomes faster after exceeding 3.5 mW/cm^2 indicating increased role of bimolecular carrier recombination. Consequently, these measurements show that all discussed nonlinear processes are insignificant at excitation intensities below 3.5 mW/cm^2. Similar results were also obtained for other investigated solar cells, thus laser intensity of 2.5 mW/cm^2 was used to avoid nonlinearities in all below discussed investigations.

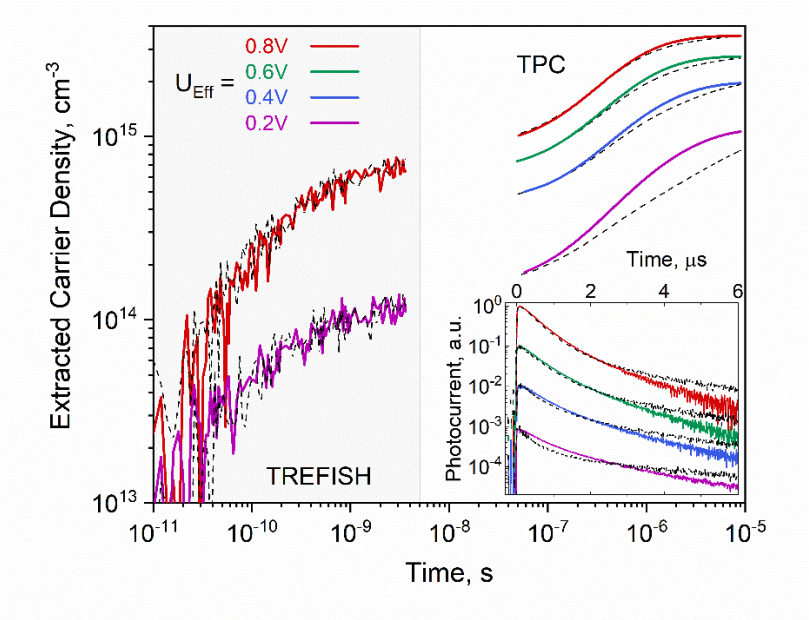

Figure 2. *Extracted laser-carrier dynamics in TQ1:PC$_{71}$BM device at various effective voltages in dark (black dashed lines) and under 1 sun illumination (color lines). Here, and in all following*

measurements, 515 nm laser excitation at 432 Hz repetition rate and ~2.5 mW/cm^2 average power was used. In the inset, photocurrent transients were normalized and vertically shifted.

Figure 2 shows charge carrier extraction dynamics from TQ1:$PC_{71}BM$ blend in a wide temporal window evaluated from measurements performed without and under additional 1 sun illumination (further referred as "dark" and 1 sun light conditions, respectively). The measurements "in dark" revealed qualitatively similar carrier extraction dynamics as was reported in ref. 18, which was evaluated as dispersive with a strongly time-dependent mobility. Decay of the carrier mobility by at least one order of magnitude during initial several nanoseconds has been observed in several polymer-PCBM blends[17–20], including TQ1:$PC_{71}BM$ blend[18] and has been attributed to the energy relaxation within the DOS. For the given sample, carrier extraction at time below 10^{-8} s is slightly suppressed, which we attribute to the charge carrier trapping that we aim to study.

In case of additional 1 sun illumination, it generated sun-carriers continuously, while their concentration was determined by the balance between extraction, recombination, and generation rates. Additional carriers generated by laser pulses (laser-carriers) now appear on a background of sun-carriers. The sun-carriers also create a constant current background, which was subtracted from our data to register photocurrent created by laser-carriers only. Importantly, additional 1 sun illumination alters the conditions under which laser-carriers are generated. First, sun-carriers fill low-energy states, therefore laser-carriers experience less trapping during their extraction from the active layer. Second, laser-carriers recombine with sun-carriers. Thus, by using two, "dark" and 1 sun light, measurement conditions, we compare carrier dynamics when a) non-geminate recombination is negligible and low-energy states are not occupied (due to low laser-carrier density, as discussed above), and b) in the presence of sun-carriers, which to some extent occupy

low-energy states. We shall inquire how 1 sun illumination affects charge extraction on different time scales at different effective electric field strengths.

As the left-hand part of Figure 2 shows, the 1 sun illumination does not change the ultrafast carrier extraction and, thus, the mobility dynamics. It indicates that sun-carriers populating low-energy states have no impact on the initial laser-carrier drift. This is expected because laser-carriers in this time-domain still reside in high-energy part of DOS and population of low-energy states by sun-carriers plays nonessential role to their dynamics. This allows us to conclude that individual charge carriers generated by sun light in real solar cells operation conditions also experience identical fast mobility decay on a ps-ns time scale as reported in previous publications[18,34].

The right-hand side of Fig. 2 shows carrier extraction dynamics obtained by integrating transient photocurrents shown in the inset. Notably, as the inset shows, the charge extraction at low U_{Eff} = 0.2V, is faster during initial 1-2 μs in the presence of 1 sun light. It signifies that laser-carriers experience weaker decay of mobility because low-energy states are significantly populated under 1 sun light. The 1 sun light influence becomes less pronounced at higher effective voltages. This is reasonable since higher voltages extract charge carriers more rapidly, including those residing in the low-energy states, liberating these states. Consequently, occupation of the low-energy states by 1 sun light decreases with voltage and weakly affects trapping of laser-carriers already at U_{Eff} = 0.4V. At longer 2-6 μs times the photocurrent decays faster under 1 sun light. This decay phase was attributed to the extraction of equilibrated carriers, thus faster photocurrent decay indicates faster decay of the carrier density, which we attribute to the SRH recombination of laser-carriers with trapped sun-carriers (second term in eq. 2).

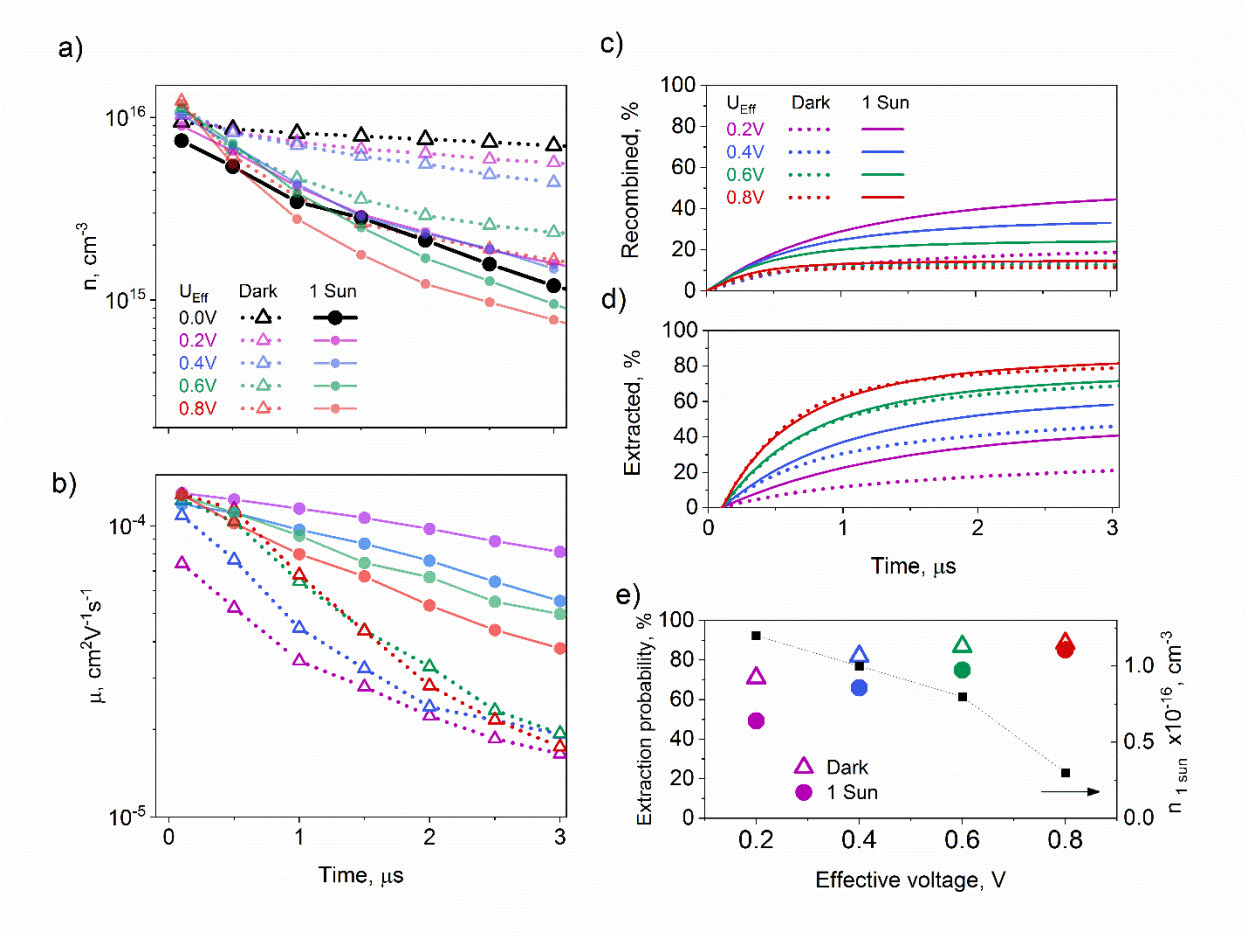

Figure 3. *a) Charge carrier density kinetics at different effective voltages in TQ1:PC$_{71}$BM device determined by TDCF measurements. Here and in all plots, solid lines correspond to measurements under 1 sun, dotted lines – "in dark"; b) carrier mobility dynamics evaluated from TDCF data and TPC data presented in Figure 2; Modelled fraction of recombined (c) and extracted (d) charge carriers; e) Carrier extraction probabilities (color symbols) "in dark" and under 1 sun, and sun-carrier density (black symbols) as functions of effective voltage.*

To quantify the influence of 1 sun illumination on bimolecular carrier recombination losses, we have performed TPC measurements in complementary time-delayed collection field implementation. As explained in the experimental section, it enables tracking of laser-carrier density kinetics, which is shown in Fig.3a. At zero effective voltage (black dotted curve), photogenerated carriers are not extracted, and their density decays due to recombination only. It allows evaluation of bimolecular recombination rate, which in this case was found being equal to

γ = 1,24x10^{-11} cm^3s^{-1}, similar to values reported elsewhere [30,31]. Increasing the effective voltage leads to more rapid carrier density decay due to carrier extraction. The clear difference between carrier density dynamics "in dark" and under 1 sun illumination (dotted and solid curves, accordingly) at zero effective voltage supports the idea of pronounced recombination of laser-carriers with sun-carriers. Noteworthy, the difference in kinetics is much smaller at higher voltages, because enhanced extraction causes smaller trapped sun-carrier population.

Combining *j(t)* obtained from TPC measurements and *n(t)* obtained from TDCF, we can evaluate the mean time-dependent carrier mobility from relation $j(t) = e\,Fn(t)\mu(t)$. The obtained mobility dynamics at different voltages "in dark" and under 1 sun light are presented in Figure 3b. The mobility is higher, and its decay is weaker under 1 sun illumination. "In dark", the mobility increases at higher voltages as typically observed in disordered organic semiconductors[35]. Slightly stronger mobility decay at high voltages is caused by faster extraction of nontrapped carriers leaving only low-mobility trapped carriers at longer times. Under 1 sun illumination, the mobility becomes less time-dependent, particularly at low effective electric field when low-energy states are populated by sun-carriers (as shown in scheme 1) preventing trapping of laser-carriers. However, population of low-energy states by sun-carriers decreases with increasing electric field, promoting trapping of laser-carriers and causing a stronger decrease of their mobility. Consequently, mobility decreases with electric field, in stark contrast with typically reported behavior.

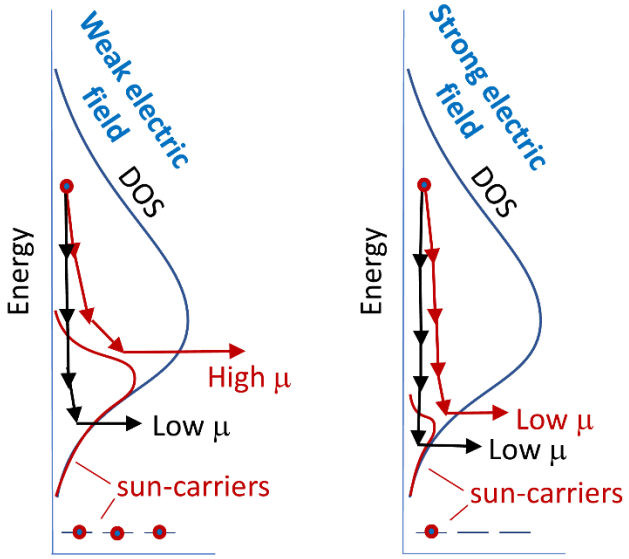

Scheme 1. *Schematic representation of charge carrier relaxation within DOS "in dark" (blue arrows) and under Solar illumination (red arrows) at low and high effective electric field values.*

It should also be noted that the population of low-energy states and its influence is expected to be less distinct at lower illumination intensities. Therefore, significant impact of trapped sun-carriers on the carrier extraction dynamics is expected only at full 1.5AM solar illumination.

To evaluate the role of the low-energy state occupation on the solar cell performance more clearly, we have performed numerical modelling of the carrier extraction and recombination processes on basis of the experimental results. A detailed description of our model is presented in experimental section, whereas fitted curves are presented in the S.I. Our numerical model provided us with total bimolecular recombination (between laser-laser and 1 sun-laser carriers combined) and carrier extraction dynamics. The "dark" conditions approximately represent the carrier extraction and recombination kinetics at constant low intensity illumination of a solar cell. As shown in Fig.3 c and d, carrier recombination dynamics at these conditions is weakly dependent on the effective voltage, while the extraction rate approximately linearly increases with voltage. At 1 sun illumination, the recombination rate strongly increases at low effective voltages because

of high density of carriers trapped in low-energy states (Fig.3c and 3e). On the other hand, the dependence of the carrier extraction on effective voltage is weaker than “in dark”. Figure 3e summarizes the calculation results. It shows that the sun-carrier concentration decreases almost four times when the effective voltage increases from 0.2V, which is close to the MPP conditions, to 0.8V, which corresponds to short-circuit. Figure 3e also shows the total probability for the generated carrier to be extracted, rather than to recombine. The carrier extraction probability under 1 sun light is lower than “in dark” because of the increased recombination rate in presence of sun-carriers, but this difference decreases with effective voltage when the density of trapped sun-carriers decreases. It should be noted that at 1 sun illumination conditions, the extraction probabilities for laser-carriers and sun-carriers are approximately equal because recombination between two laser-carriers is insignificant at low laser-carrier concentration.

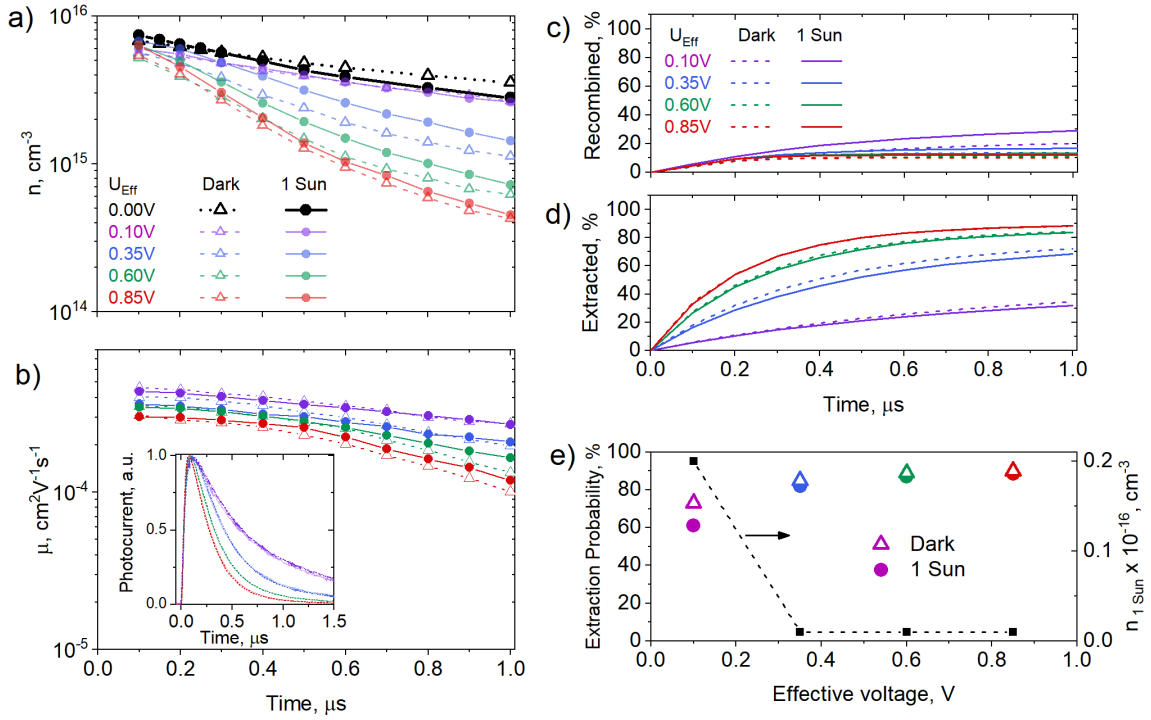

Figure 4. *Carrier density (a) and mobility (b) kinetics in PBDB-T:Y1 device obtained from TPC and TDCF measurements combined. Inset in (b) shows normalized photocurrent kinetics. Modeled recombination (c) and extraction (d) dynamics. e) Carrier extraction probabilities (color symbols) "in dark"and under 1 sun, and sun-carrier density (black symbols) as functions of effective voltage.*

An analogous analysis of the carrier dynamics on a microsecond time scale was performed on effective (PCE = 13.2%) non-fullerene acceptor (NFA) device PBDB-T:Y1 (Fig.4a-e). Photocurrent decay in NFA sample was faster than in the present TQ1:$PC_{71}BM$ blend. For instance, at 0.8V voltage 1μs after excitation, only 3% of the initial photocurrent value was present in the PBDB-T:Y1 device, (Fig.4b inset) compared to 30% in TQ1:$PC_{71}BM$ sample with increased carrier trapping. It signifies that either carrier recombination or extraction, or both, are much faster in the PBDB-T:Y1 device. Secondly, there is no rapid photocurrent decay "in dark" at low voltages that was clearly expressed in TQ1:$PC_{71}BM$ and that we attributed to the carrier trapping. It shows that carrier trapping in PBDB-T:Y1 is not a dominant factor determining photocurrent decay on a

submicrosecond time scale. Thirdly, differences between photocurrent kinetics “in dark” and under 1 sun light are insignificant at all applied voltages. It shows that the sun-carrier concentration is minute at any voltage, again suggesting relative scarcity of low-energy states or their shallow depth in this device.

Furthermore, TDCF measurements show that carrier density and mobility kinetics are only weakly affected by 1 sun illumination (Fig. 4 b-c) and depend only on effective voltage. It shows that low-energy state occupation by sun-carriers does not affect the drift of laser-carriers. Also, in these devices, the carrier mobility decreases with effective voltage, but to a lesser extent than in the TQ1:$PC_{71}BM$ blend. This further illustrates the fact that carrier mobility is not a perfect parameter to characterize carrier motion in organic solar cells. In these experiments, the effective carrier mobility decreases with voltage because highly mobile charge carriers are extracted from the sample, leaving low mobility carriers relaxed to deep tail states within the DOS. The fraction of extracted highly mobile carriers increases with time and effective voltage. At high effective voltages, highly mobile carriers are extracted faster than the time-resolution of our TDCF measurements, thus already at 100 ns, our technique probes a reduced carrier mobility. The data obtained at low U_{Eff} is less affected by this effect and represents the behavior of the dominating fraction of carriers more correctly. Nevertheless, even at low effective voltages of 0.1V and 0.35V, i.e. close to MPP of the solar cell, the carrier mobility still decreases by about 30-50% in the sub-μs time scale both ”in dark” and at 1 sun illumination. This minor but significant decrease is consistent with the concept of a nearly constant mobility for this time range. Note, however, that significant (dispersive) extraction can take place at shorter time scales as further discussed below[28,29].

Computational modelling shows that at close to MPP voltages, sun-carrier concentration in PBDB-T:Y1 device is indeed lower by one order of magnitude than in the here investigated TQ1:$PC_{71}BM$ device. Even though TDCF measurements at U_{Eff} = 0V gives bimolecular recombination rate of $\gamma = 2.2x10^{-10}cm^3s^{-1}$ for the PBDB-T:Y1 sample, which is significantly higher than in the TQ1:$PC_{71}BM$ device, the lower carrier concentration still leads to a weak enhancement of non-geminate recombination in the presence of sun-carriers (Fig.4d). Even at the lowest effective voltage of 0.1V, when carrier extraction is relatively slow, non-geminate recombination losses increase no more than 10% in the presence of 1 sun illumination. Moreover, a few times higher mobility values compared to TQ1:$PC_{71}BM$ device, leads to much faster and more effective carrier extraction, as shown in Fig. 4e.

Ultrafast TREFISH investigations were not possible for this device because of significantly lower second harmonic generation efficiency in the non-fullerene blend. However, previous investigations performed by an alternative, ultrafast time-resolved electroabsorption technique, revealed mobility decrease “in dark” by more than an order of magnitude during an initial couple of nanoseconds.[17] Taking into account that mobility on this ultrafast time scale was independent of the 1 sun illumination even in the TQ1:$PC_{71}BM$ blend, where the influence of illumination on the microsecond mobility was much stronger, we do not expect any significant illumination influence on the ultrafast mobility in the PBDB-T:Y1 blend as well. Consequently, these data allow us to conclude that the carrier mobility in PBDB-T:Y1 solar cell in real operation conditions is strongly time-dependent on the ps-ns time scale.

Investigations of the TQ1:$PC_{71}BM$ and PBDB-T:Y1 blends have shown that precise measurements of transient photocurrent kinetics at low laser intensity performed “in dark” and

under 1 sun illumination are sufficient to estimate the role of a low-energy state population on the carrier extraction.

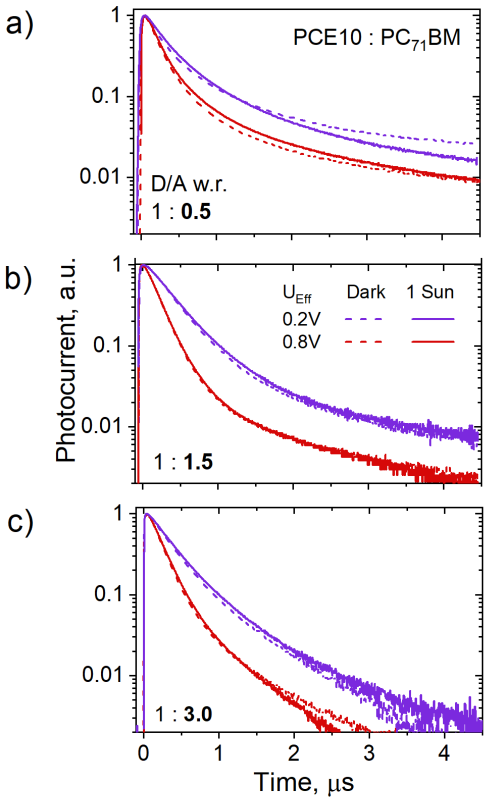

Figure 5. *Transient photocurrent kinetics at 0.2V (red curves) and 0.8V (purple curves) effective voltage, "in dark"(dotted lines) and sun-light (lines lines) conditions, for PCE10:$PC_{71}BM$ samples a) 0.5; b) 1.5 and c) 3.0.*

To consider the role of blend morphology on the formation and properties of low-energy states, we have also performed TPC measurements on three different devices based on the efficient donor polymer PCE10 and the $PC_{71}BM$ acceptor, mixed at different D/A weight ratios of 1:0.5, 1:1.5 and 1:3, (further referred to as sample **0.5**, **1.5** and **3.0**, accordingly). As shown in the Table presented

in Fig.S1, the optimal concentration was 1:1.5, which resulted in PCE of 6.5% and the highest values of other photovoltaic parameters.

Carrier motion dynamics in fullerene-based solar cells was found to be strongly dependent on the stoichiometric ratio of donor and acceptor materials[36]. The slow carrier extraction component at $t > 1$ μs clearly decreases at higher $PC_{71}BM$ concentration, and therefore can be attributed to the electron extraction via $PC_{71}BM$ domains, which may lose percolation pathways at low $PC_{71}BM$ concentration, causing the formation of dead ends in the electron transfer pathways[7]. The current TPC investigation results (Figure 5 a-c) agree with this conception. At low $PC_{71}BM$ concentration (sample **0.5**), the TPC kinetics is qualitatively similar to that obtained for TQ1:$PC_{71}BM$ sample indicating the increased density of low-energy states, which are occupied under 1 sun illumination. However, TPC kinetic in samples **1.5** and **3.0** show almost no influence of the 1 sun illumination, similarly to the PBDB-T:Y1 blend, suggesting that carrier trapping and occupation of low-energy states by 1 sun illumination are marginal. Considering that chemical structures and fabrication procedures of all PCE10:$PC_{71}BM$ samples were identical, the more expressed influence of low-energy states in the sample with low $PC_{71}BM$ concentration suggests that especially dead ends in the electron pathways create additional traps, causing a significant slowing of electron extraction. Note that we cannot exclude that the low-energy states in the investigated TQ1:PCBM blend are also to some degree geometrical in nature, although geometrical trapping is normally weak in this system due to the presence of a significant fraction of fullerene in the donor-rich phase [10,42].

Conclusions

In conclusion, we have addressed the role of population of low-energy states on carrier dynamics in organic solar cells operating in quasi-real conditions. We applied several transient methods to cover a wide temporal window from picoseconds to microseconds and analysed the influence of

solar illumination on carrier mobility, extraction and recombination. Carrier trapping strongly influences the carrier mobility on a ns - μs time scale in TQ1:$PC_{71}BM$ devices possessing deep low-energy states, but steady-state solar illumination causes occupation of these state, making the carrier mobility less time-dependent. At low electric fields, close to the MPP conditions, the low-energy state filling increases both recombination and extraction rates and reduces the extraction efficiency. However, low-energy state population becomes less significant and weakly affects carrier dynamics when the internal electric field is sufficiently strong, which happens close to short-circuit conditions. On the other hand, low-energy state filling does not affect the strongly decreasing mobility on a ps-time scale.

Carrier trapping plays less significant role in more effective solar cells. Carrier mobility in non-fullerene PBDB-T:Y1 solar cell is weakly time-dependent on a ns to μs time scale and low-energy state filling by solar illumination plays only a marginal role, even at low, close to MPP effective voltages. Carrier trapping in PCE10:$PC_{71}BM$ solar cells with different donor/acceptor stoichiometric ratios was found to be more significant at low PCBM concentrations, when poor PCBM domain percolation caused the formation of geometrical electron traps.

The investigation results also show that carrier mobility is strongly time-dependent on a ps-ns time scale during carrier relaxation within high energy states of DOS in all investigated organic solar cells, independently of the occupation of low-energy states by solar illumination. While at longer times, occupation of low-energy states significantly changes charge carrier mobility and recombination rate in cells with increased carrier trapping, but its influence was found being only marginal in efficient solar cells.

ACKNOWLEDGMENT

We are grateful to Armantas Milianas for inspiring discussions. T. U. gratefully acknowledges funding by Vetenskapsrådet, project “OPV2.0”. M. K. thanks the Carl Zeiss Foundation for financial support.

ASSOCIATED CONTENT

Supporting Information Available: Materials, device fabrication, photovoltaic characteristics, measurements schemes, model fits.

REFERENCES:

(1) Inganäs, O. Organic Photovoltaics over Three Decades. *Adv. Mater.* **2018**, *30* (35), 1800388.

(2) Zhu, L.; Zhang, M.; Zhou, G.; Hao, T.; Xu, J.; Wang, J.; Qiu, C.; Prine, N.; Ali, J.; Feng, W., et al. Efficient Organic Solar Cell with 16.88% Efficiency Enabled by Refined Acceptor Crystallization and Morphology with Improved Charge Transfer and Transport Properties. *Adv. Energy Mater.* **2020**, *10* (18), 1904234.

(3) Cui, Y.; Yao, H.; Zhang, J.; Zhang, T.; Wang, Y.; Hong, L.; Xian, K.; Xu, B.; Zhang, S.; Peng, J., et al. Over 16% Efficiency Organic Photovoltaic Cells Enabled by a Chlorinated Acceptor with Increased Open-Circuit Voltages. *Nat. Commun.* **2019**, *10* (1), 2515.

(4) Mandoc, M. M.; Kooistra, F. B.; Hummelen, J. C.; de Boer, B.; Blom, P. W. M. Effect of Traps on the Performance of Bulk Heterojunction Organic Solar Cells. *Appl. Phys. Lett.* **2007**, *91* (26), 263505.

(5) Venkateshvaran, D.; Nikolka, M.; Sadhanala, A.; Lemaur, V.; Zelazny, M.; Kepa, M.; Hurhangee, M.; Kronemeijer, A. J.; Pecunia, V.; Nasrallah, I., et al. Approaching Disorder-Free Transport in High-Mobility Conjugated Polymers. *Nature* **2014**, *515* (7527), 384–388.

(6) Wu, J.; Lee, J.; Chin, Y.-C.; Yao, H.; Cha, H.; Luke, J.; Hou, J.; Kim, J.-S.; Durrant, J. R. Exceptionally Low Charge Trapping Enables Highly Efficient Organic Bulk Heterojunction Solar Cells. *Energy Environ. Sci.* **2020**, *13* (8), 2422–2430.

(7) Melianas, A.; Etzold, F.; Savenije, T. J.; Laquai, F.; Inganäs, O.; Kemerink, M. Photo-Generated Carriers Lose Energy during Extraction from Polymer-Fullerene Solar Cells. *Nat. Commun.* **2015**, *6*.

(8) Wu, J.; Luke, J.; Lee, H. K. H.; Shakya Tuladhar, P.; Cha, H.; Jang, S.-Y.; Tsoi, W. C.; Heeney, M.; Kang, H.; Lee, K., et al. Tail State Limited Photocurrent Collection of Thick Photoactive Layers in Organic Solar Cells. *Nat. Commun.* **2019**, *10* (1), 5159.

(9) Fischer, J.; Ray, D.; Kleemann, H.; Pahner, P.; Schwarze, M.; Koerner, C.; Vandewal, K.; Leo, K. Density of States Determination in Organic Donor-Acceptor Blend Layers Enabled by Molecular Doping. *J. Appl. Phys.* **2015**, *117* (24), 245501.

(10) Jasiūnas, R.; Melianas, A.; Xia, Y.; Felekidis, N.; Gulbinas, V.; Kemerink, M. Dead Ends Limit Charge Carrier Extraction from All-Polymer Bulk Heterojunction Solar Cells. *Adv. Electron. Mater.* **2018**, *4* (8), 1800144.

(11) Cha, H.; Wu, J.; Wadsworth, A.; Nagitta, J.; Limbu, S.; Pont, S.; Li, Z.; Searle, J.; Wyatt, M. F.; Baran, D., et al. An Efficient, "Burn in" Free Organic Solar Cell Employing a Nonfullerene Electron Acceptor. *Adv. Mater.* **2017**, *29* (33), 1701156.

(12) Moses, D.; Sinclair, M.; Heeger, A. J. Carrier Photogeneration and Mobility in Polydiacetylene: Fast Transient Photoconductivity. *Phys. Rev. Lett.* **1987**, *58* (25), 2710–2713.

(13) Bässler, H. Charge Transport in Disordered Organic Photoconductors a Monte Carlo Simulation Study. *Phys Status Solidi B* **1993**, *175* (1), 15–56.

(14) Devižis, A.; Meerholz, K.; Hertel, D.; V. Gulbinas. Hierarchical Charge Carrier Motion in Conjugated Polymers. *Chem. Phys. Lett.* **2010**, 5.

(15) Devizis, A.; Meerholz, K.; Hertel, D.; Gulbinas, V. Ultrafast Charge Carrier Mobility Dynamics in Poly(Spirobifluorene- c o -Benzothiadiazole): Influence of Temperature on Initial Transport. *Phys. Rev. B* **2010**, *82* (15), 155204.

(16) Devižis, A.; Serbenta, A.; Meerholz, K.; Hertel, D.; Gulbinas, V. Ultrafast Dynamics of Carrier Mobility in a Conjugated Polymer Probed at Molecular and Microscopic Length Scales. *Phys. Rev. Lett.* **2009**, *103* (2), 027404.

(17) Jasiunas, R.; Zhang, H.; Yuan, J.; Zhou, X.; Qian, D.; Zou, Y.; Devižis, A.; Sulskus, J.; Gao, F.; Gulbinas, V. From Generation to Extraction: A Time-Resolved Investigation of Photophysical Processes in Non-Fullerene Organic Solar Cells. *J. Phys. Chem. C* **2020**, 124, 39, 21283–21292.

(18) Melianas, A.; Pranculis, V.; Devižis, A.; Gulbinas, V.; Inganäs, O.; Kemerink, M. Dispersion-Dominated Photocurrent in Polymer:Fullerene Solar Cells. *Adv. Funct. Mater.* **2014**, *24* (28), 4507–4514.

(19) Abramavičius, V.; Amarasinghe Vithanage, D.; Devižis, A.; Infahsaeng, Y.; Bruno, A.; Foster, S.; Keivanidis, P. E.; Abramavičius, D.; Nelson, J.; Yartsev, A., et al. Carrier Motion in As-Spun and Annealed P3HT:PCBM Blends Revealed by Ultrafast Optical Electric Field Probing and Monte Carlo Simulations. *Phys. Chem. Chem. Phys.* **2014**, *16* (6), 2686.

(20) Augulis, R.; Devižis, A.; Peckus, D.; Gulbinas, V.; Hertel, D.; Meerholz, K. High Electron Mobility and Its Role in Charge Carrier Generation in Merocyanine/Fullerene Blends. *J. Phys. Chem. C* **2015**, *119* (11), 5761–5770.

(21) Cunningham, P. D.; Hayden, L. M. Carrier Dynamics Resulting from Above and Below Gap Excitation of P3HT and P3HT/PCBM Investigated by Optical-Pump Terahertz-Probe Spectroscopy. *J. Phys. Chem. C* **2008**, *112* (21), 7928–7935.

(22) Ai, X.; Beard, M. C.; Knutsen, K. P.; Shaheen, S. E.; Rumbles, G.; Ellingson, R. J. Photoinduced Charge Carrier Generation in a Poly(3-Hexylthiophene) and Methanofullerene Bulk Heterojunction Investigated by Time-Resolved Terahertz Spectroscopy. *J. Phys. Chem. B* **2006**, *110*, 50, 25462–25471.

(23) Ponseca, C. S.; Yartsev, A.; Wang, E.; Andersson, M. R.; Vithanage, D.; Sundström, V. Ultrafast Terahertz Photoconductivity of Bulk Heterojunction Materials Reveals High Carrier Mobility up to Nanosecond Time Scale. *J. Am. Chem. Soc.* **2012**, *134* (29), 11836–11839.

(24) Mihailetchi, V. D.; Xie, H. X.; de Boer, B.; Koster, L. J. A.; Blom, P. W. M. Charge Transport and Photocurrent Generation in Poly(3-Hexylthiophene): Methanofullerene Bulk-Heterojunction Solar Cells. *Adv. Funct. Mater.* **2006**, *16* (5), 699–708.

(25) Bartelt, J. A.; Lam, D.; Burke, T. M.; Sweetnam, S. M.; McGehee, M. D. Charge-Carrier Mobility Requirements for Bulk Heterojunction Solar Cells with High Fill Factor and External Quantum Efficiency >90%. *Adv. Energy Mater.* **2015**, *5* (15), 1500577.

(26) Bartesaghi, D.; Pérez, I. del C.; Kniepert, J.; Roland, S.; Turbiez, M.; Neher, D.; Koster, L. J. A. Competition between Recombination and Extraction of Free Charges Determines the Fill Factor of Organic Solar Cells. *Nat. Commun.* **2015**, *6* (1), 7083.

(27) Proctor, C. M.; Love, J. A.; Nguyen, T.-Q. Mobility Guidelines for High Fill Factor Solution-Processed Small Molecule Solar Cells. *Adv. Mater.* **2014**, *26* (34), 5957–5961.

(28) Le Corre, V. M.; Chatri, A. R.; Doumon, N. Y.; Koster, L. J. A. Charge Carrier Extraction in Organic Solar Cells Governed by Steady-State Mobilities. *Adv. Energy Mater.* **2017**, *7* (22), 1701138.

(29) Felekidis, N.; Melianas, A.; Aguirre, L. E.; Kemerink, M. Comment on "Charge Carrier Extraction in Organic Solar Cells Governed by Steady-State Mobilities." *Adv Energy Mater* **2018**, 8, 1800419.

(30) Karuthedath, S.; Gorenflot, J.; Melianas, A.; Kan, Z.; Kemerink, M.; Laquai, F. Buildup of Triplet-State Population in Operating TQ1:PC $_{71}$ BM Devices Does Not Limit Their Performance. *J. Phys. Chem. Lett.* **2020**, *11* (8), 2838–2845.

(31) Andersson, L. M.; Melianas, A.; Infahasaeng, Y.; Tang, Z.; Yartsev, A.; Inganäs, O.; Sundström, V. Unified Study of Recombination in Polymer:Fullerene Solar Cells Using Transient Absorption and Charge-Extraction Measurements. *J. Phys. Chem. Lett.* **2013**, *4* (12), 2069–2072.

(32) Roland, S.; Kniepert, J.; Love, J. A.; Negi, V.; Liu, F.; Bobbert, P.; Melianas, A.; Kemerink, M.; Hofacker, A.; Neher, D. Equilibrated Charge Carrier Populations Govern Steady-State Nongeminate Recombination in Disordered Organic Solar Cells. *J. Phys. Chem. Lett.* **2019**, *10* (6), 1374–1381.

(33) Li, S.; Li, C.-Z.; Shi, M.; Chen, H. New Phase for Organic Solar Cell Research: Emergence of Y-Series Electron Acceptors and Their Perspectives. *ACS Energy Lett.* **2020**, *5* (5), 1554–1567.

(34) Gulbinas, V. Charge Carrier Mobility Dynamics in Organic Semiconductors and Solar Cells. *Lith. J. Phys.* **2020**, *60* (1).

(35) Upreti, T.; Wang, Y.; Zhang, H.; Scheunemann, D.; Gao, F.; Kemerink, M., Experimentally Validated Hopping-Transport Model for Energetically Disordered Organic Semiconductors, *Phys. Rew. Appl.* **2019,** 12,064039.

(36) Pranculis, V.; Infahsaeng, Y.; Tang, Z.; Devižis, A.; Vithanage, D. A.; Ponseca, C. S.; Inganäs, O.; Yartsev, A. P.; Gulbinas, V.; Sundström, V. Charge Carrier Generation and Transport in Different Stoichiometry APFO3:PC61BM Solar Cells. *J. Am. Chem. Soc.* **2014**, *136* (32), 11331–11338.

(37) Yuan, J.; Huang, T.; Cheng, P.; Zou, Y.; Zhang, H.; Yang, J. L.; Chang, S.-Y.; Zhang, Z.; Huang, W.; Wang, R., et al. Enabling Low Voltage Losses and High Photocurrent in Fullerene-Free Organic Photovoltaics. *Nat. Commun.* **2019**, *10* (1), 570.

(38) Hou, J.; Inganäs, O.; Friend, R. H.; Gao, F. Organic Solar Cells Based on Non-Fullerene Acceptors. *Nat. Mater.* **2018**, *17* (2), 119–128.

(39) Cheng, P.; Li, G.; Zhan, X.; Yang, Y. Next-Generation Organic Photovoltaics Based on Non-Fullerene Acceptors. *Nat. Photonics* **2018**, *12* (3), 131–142.

(40) Perdigón-Toro, L.; Zhang, H.; Markina, A.; Yuan, J.; Hosseini, S. M.; Wolff, C. M.; Zuo, G.; Stolterfoht, M.; Zou, Y.; Gao, F.; Andrienko, D., et al. Barrierless Free Charge Generation in the High-Performance PM6:Y6 Bulk Heterojunction Non-Fullerene Solar Cell. *Adv. Mater.* **2020**, *32* (9), 1906763.

(41) Kurpiers, J.; Neher, D. Dispersive Non-Geminate Recombination in an Amorphous Polymer:Fullerene Blend. *Sci. Rep.* **2016**, *6* (1).

(42) Wilken, S.; Upreti, T.; Melianas, A.; Dahlström, S.; Persson, G.; Olsson, E.; Österbacka, R.; Kemerink, M. Experimentally Calibrated Kinetic Monte Carlo Model Reproduces Organic Solar Cell Current–Voltage Curve. *Sol. RRL* **2020**, 4 (6), 2000029.

ToC